



HAL
open science

Cold Dense Ion Outflow Observed in the Martian-Induced Magnetotail by MAVEN

S. Inui, K. Seki, T. Namekawa, S. Sakai, D. A. Brain, T. Hara, J. P.
Mcfadden, J. S. Halekas, D. L. Mitchell, C. Mazelle, et al.

► **To cite this version:**

S. Inui, K. Seki, T. Namekawa, S. Sakai, D. A. Brain, et al.. Cold Dense Ion Outflow Observed in the Martian-Induced Magnetotail by MAVEN. *Geophysical Research Letters*, 2018, 45, pp.5283-5289. 10.1029/2018GL077584 . insu-03678199

HAL Id: insu-03678199

<https://insu.hal.science/insu-03678199>

Submitted on 25 May 2022

HAL is a multi-disciplinary open access archive for the deposit and dissemination of scientific research documents, whether they are published or not. The documents may come from teaching and research institutions in France or abroad, or from public or private research centers.

L'archive ouverte pluridisciplinaire **HAL**, est destinée au dépôt et à la diffusion de documents scientifiques de niveau recherche, publiés ou non, émanant des établissements d'enseignement et de recherche français ou étrangers, des laboratoires publics ou privés.

Copyright

RESEARCH LETTER

10.1029/2018GL077584

Key Points:

- Cold dense heavy ion outflow was observed by MAVEN in the southern downward E_{sw} quadrant of the Martian-induced magnetotail
- CO_2^+ number density estimated by a fitting method to eliminate O_2^+ contamination accounts for about 3% of the total heavy ion outflow
- The ratio of $O_2^+ : O^+ : CO_2^+$ suggests that the source altitude of heavy ion outflow was around 260 km or below in the Martian ionosphere

Correspondence to:

S. Inui,
inui@eps.s.u-tokyo.ac.jp

Citation:

Inui, S., Seki, K., Namekawa, T., Sakai, S., Brain, D. A., Hara, T., et al. (2018). Cold dense ion outflow observed in the Martian-induced magnetotail by MAVEN. *Geophysical Research Letters*, 45, 5283–5289. <https://doi.org/10.1029/2018GL077584>

Received 15 FEB 2018

Accepted 14 MAY 2018

Accepted article online 21 MAY 2018

Published online 5 JUN 2018

Cold Dense Ion Outflow Observed in the Martian-Induced Magnetotail by MAVEN

S. Inui¹ , K. Seki¹ , T. Namekawa¹ , S. Sakai¹ , D. A. Brain² , T. Hara³ , J. P. McFadden³,
J. S. Halekas⁴ , D. L. Mitchell³ , C. Mazelle⁵ , G. A. DiBraccio⁶ , and B. M. Jakosky² 

¹Department of Earth and Planetary Science, Graduate School of Science, University of Tokyo, Tokyo, Japan,

²Laboratory for Atmospheric and Space Physics, University of Colorado Boulder, Boulder, CO, USA, ³Space Sciences Laboratory, University of California, Berkeley, CA, USA, ⁴Department of Physics and Astronomy, University of Iowa, Iowa City, IA, USA, ⁵IRAP, University of Toulouse, CNRS, UPS, CNES, Toulouse, France, ⁶NASA Goddard Space Flight Center, Greenbelt, MD, USA

Abstract Cold ion outflow is one of the candidate processes to cause significant atmospheric escape from Mars. We here report on the cold dense heavy ion outflow event observed in Martian-induced magnetotail by Mars Atmosphere and Volatile Evolution (MAVEN) on 4 December 2014. In the outflow event, the cold dense heavy ion outflow was observed only in south dusk downward convection electric field (E) lobe. During the event, the strong crustal magnetic field was located on dayside of Mars. It suggests that combination of minimagnetosphere and downward E facilitates the cold dense heavy ion outflow. In order to estimate the CO_2^+ density, we adopted a fitting method of log-normal distribution to the O_2^+ time of flight distributions to eliminate O_2^+ contamination in the CO_2^+ time of flight data. Contribution of O_2^+ , O^+ , and CO_2^+ to the total heavy ions ($\sim 134 \text{ cm}^{-3}$) is about 71%, 26%, and 3%, respectively. Average heavy ion flux was $\sim 5.4 \times 10^7 \text{ cm}^{-2} \text{ s}^{-1}$, assuming the escape velocity at 2,000-km altitude.

Plain Language Summary Mars has a cold surface temperature and little water on surface at present. However, it is thought that Mars had a warm climate and liquid water on surface about 4 billion years ago. In order to cause the climate change, a large amount of CO_2 , that is, greenhouse gas, needs to be removed from Martian atmosphere. While the ion escape from the Martian upper atmosphere to space through interaction between the solar wind and Mars is one of the candidate mechanisms to remove CO_2 , detailed characteristics of the ion escape such as its composition and relation to the solar wind conditions are far from understood. Based on observations in the Martian-induced magnetotail by the Mars Atmosphere and Volatile Evolution mission, we here report on the cold dense heavy ion outflow event which accounts for a significant escape flux. A careful analysis enables us to derive densities of O^+ , O_2^+ , and CO_2^+ ions separately. The resultant ion species ratio suggests the ion escape from deep ionosphere below altitudes of 300 km. Observations also indicate that both the solar wind electric field and the crustal magnetic fields play an important role to cause the cold dense ion outflow.

1. Introduction

Geological studies have suggested that Mars had a warm climate and liquid water on surface about 4 billion years ago, while Mars has a cold surface temperature and little water on surface at present (e.g., Bibring et al., 2006; Jakosky & Phillips, 2001). It is thought that the warm climate on early Mars was maintained by dense atmosphere including greenhouse gases (e.g., Ramirez et al., 2014). To cause the drastic climate change, escape of greenhouse gases such as CO_2 to space is considered as the plausible reason. However, the mechanism enabling the large amount of the CO_2 loss is far from understood. The planetary ion escape through interaction between the solar wind and the Martian upper atmosphere can be one of the candidate mechanisms leading to the atmospheric escape (Chassefière & Leblanc, 2004).

Solar wind plays an important role in heavy ion escape. When the upstream solar wind dynamic pressure is strong, a large amount of heavy ions escape from Mars (Lundin et al., 2008). The upstream magnetic field strength also has an influence on the ion outflow (Nilsson et al., 2010). Moreover, Dong et al. (2015) showed that there are mainly three escape channels: antisunward fluxes in the tail region, strong plume fluxes in the direction of the solar wind convection electric field in Mars-Sun-Electric field

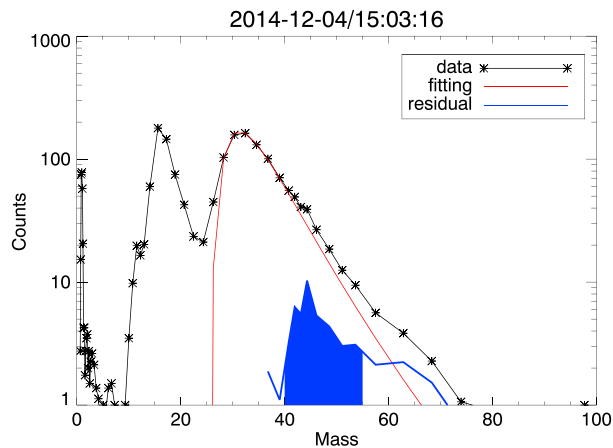


Figure 1. Example of derivation of CO_2^+ number density at 15:03:16 on 4 December 2014. Black symbols represent the data with the energy of 8.1 eV, and red line represents the fitting function for O_2^+ distribution. Blue line shows a residual between data and fitting function. The residual data in mass range from 40 to 55 (blue shaded area) are used to derive CO_2^+ number density.

coordinate (X : Sun direction, Z : solar wind electric field direction, and Y : $Z \times X$ direction), and pickup ion fluxes on the dayside. Brain et al. (2015) calculated net number fluxes of heavy ions with higher energies than 25 eV, and they obtained a lower bound estimate for planetary ion escape of about $3 \times 10^{24} \text{ s}^{-1}$.

Mars does not have global intrinsic magnetic field. However, it has local crustal magnetic fields on its surface (Acuña et al., 1999; Connerney et al., 2005). Due to the local crustal magnetic fields, escape mechanisms become complicated. Some researches considered the relationship between local crustal magnetic fields and escape rate (e.g., Brain et al., 2010; Fang et al., 2015; Lundin et al., 2011; Ramstad et al., 2016; Soobiah et al., 2006). However, we have not fully understood the role of local crustal magnetic fields in heavy ion escape yet.

The escape rate of heavy ions has been estimated by Mars Express (e.g., Barabash et al., 2007; Carlsson et al., 2006; Lundin et al., 2009; Nilsson et al., 2011). From their results, the main ion species in the heavy ion escape are inferred to be O^+ and O_2^+ , while they also reported that significant amounts of CO_2^+ escape. It is difficult to detect the cold ions precisely although it is important to assess their contribution to the total ion escape (Brain et al., 2015; Lundin et al.,

2009). The contamination of O_2^+ ions prevents us from calculating CO_2^+ number density precisely, because the mass per charge ratio of O_2^+ ions is closed to that of CO_2^+ .

In this study, we report on the cold dense heavy ion outflow event on 4 December 2014 observed by Mars Atmosphere and Volatile EvolutionN (MAVEN; Jakosky et al., 2015) in the induced magnetotail wake region. Cold ions can be detected because of negative charging of the spacecraft. Cold ions are accelerated toward the spacecraft when the spacecraft potential is negative, and we can detect the ions. We also present a method to estimate number density of CO_2^+ through subtracting O_2^+ contamination from the data, and the method is applied to the cold dense heavy ion outflow event.

2. Instrumentation and Data Analysis

2.1. Instrumentation

MAVEN has nine science instruments dedicated to understand escape processes from Mars (Lillis et al., 2015). The magnetometer (MAG; Connerney et al., 2015), the Solar Wind Ion Analyzer (SWIA; Halekas et al., 2015), and the Supra-Thermal And Thermal Ion Composition (STATIC; McFadden et al., 2015) instrument onboard MAVEN were used in our study. STATIC was used to derive density of each ion species, and MAG and SWIA were used to derive solar wind conditions and field configuration in the magnetotail. The solar wind conditions were determined by the same method as that described in Halekas et al. (2017). The energy range of STATIC is 0.1 eV to 30 keV. STATIC provides several data products, and we used “c6” data product with high resolution in mass. It has 32 energy bins and 64 mass bins. Time resolution and energy range of SWIA are 4 s and 5 eV to 25 keV, respectively. The MAG samples magnetic field vectors at a maximum rate of 32 Hz, and we use 1-s average of this data for our investigation.

2.2. Estimation of CO_2^+ Density

To estimate CO_2^+ number density precisely, subtraction of the O_2^+ contamination is needed. We first determined the response function (i.e., mass-counts relationship) of the STATIC instrument to O_2^+ ions. We selected data in which CO_2^+ contribution is small from all MAVEN orbits #1476-4854 (obtained from July 2015 to March 2017). STATIC “pickup” mode data were only used. We divided the selected data into individual energy steps and determined the response functions corresponding to each energy step by using fitting method. Note that the data with energies less than 2 eV were merged under the assumption that the response function does not depend on energies less than 2 eV.

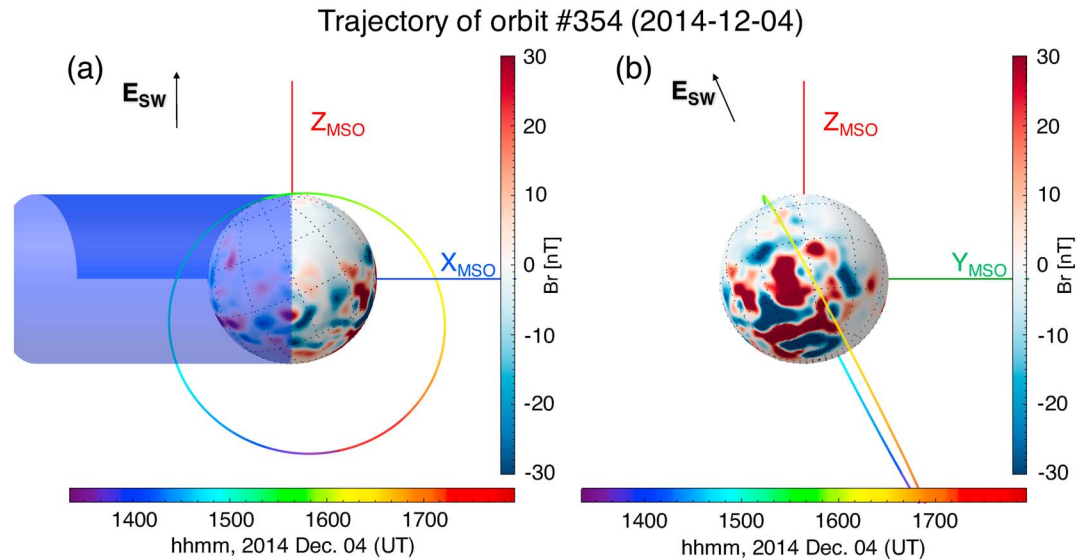


Figure 2. Trajectory map of MAVEN orbit #354 (4 December 2014), projected onto (a) the X-Z and (b) the Y-Z plane in the MSO coordinates. Blue, green, and red lines represent +X, +Y, and +Z direction in the MSO coordinates, respectively. Blue shaded region in Figure 2a shows the wake region. Red and blue colors on the Martian surface indicate the radial component of modeled crustal magnetic fields at 400 km at 15:38 (Morschhauser et al., 2014). The direction of E_{sw} (the solar wind electric field) is displayed with the black arrows in the figure. Southern and northern hemispheres roughly correspond to downward and upward E_{sw} hemispheres, respectively. MAVEN = Mars Atmosphere and Volatile Evolution.

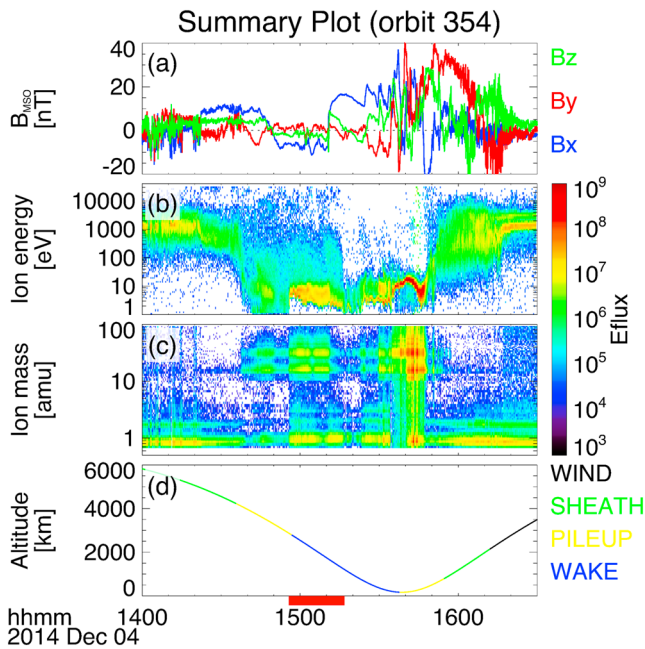


Figure 3. Summary plot of MAVEN observations in the 4 December 2014 event: (a) magnetic field in the MSO coordinates (MAG), (b) energy time, (c) mass-time spectra (STATIC) in which color codes indicate differential energy flux (“Eflux”), and (d) spacecraft altitude in which colors indicate each plasma region (Trotignon et al., 2006). Red bar at the bottom of the figure indicates the period when cold dense heavy ions were observed and corresponds to the period shown in Figure 4. MAVEN = Mars Atmosphere and Volatile Evolution; MAG = magnetometer; STATIC = Supra-Thermal And Thermal Ion Composition.

As a fitting function to the O_2^+ distribution in TOF (time of flight) data, we adopted a log-normal distribution

$$f(x) = k \frac{1}{\sqrt{2\pi\sigma}(x-c)} \exp\left[-\frac{(\ln(x-c) - \mu)^2}{2\sigma^2}\right]$$

where x represents mass per charge number and c represents translation in x direction. We determined the values of c , σ , and μ by using fitting method. Coefficient k was determined by the peak value of O_2^+ counts.

We utilized the obtained parameters of the fitting function to subtract the contamination of O_2^+ ions included in CO_2^+ TOF data bins from the 64-s resolution data. In this process, we determined the coefficient k to fit the right slope. After calculating residual counts (original data-fitting function) at each CO_2^+ TOF bin, moment calculation was conducted for the residual data in mass range from 40 to 55 (blue shade in Figure 1) to derive CO_2^+ number density since CO_2^+ ions are expected to be distributed in this mass range. Energy shift caused by the spacecraft potential was corrected in the density calculation. Spacecraft potential was obtained by the energy cutoff of the STATIC instrument, and its range is about -5.4 to -1 V in the cold ion outflow event. From Figure 1, the obtained O_2^+ distribution fits well to the data in the range of 25 to 40 by mass. When mass approaches 40, the residual between the data and obtained fitting function starts to expand. Blue shaded area (around 44 by mass) is regarded as contribution from CO_2^+ ions. We tried various fitting functions to assess their effect on the resultant CO_2^+ density. The uncertainty in the CO_2^+ density is within 10%.

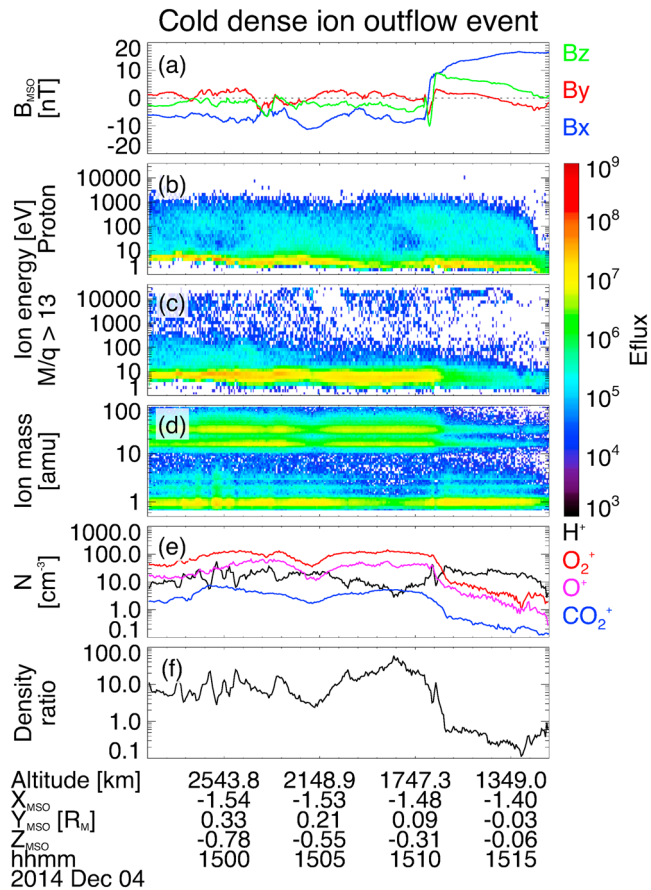


Figure 4. Summary time series plots of number densities of ions in the period indicated by red bar in Figure 3. Panels (a) and (d) are identical to panels (a) and (c) in Figure 3. Panels (b) and (c) show energy-time spectrograms for proton and heavy ions. Panel (e) shows number densities for each ion species (black: H^+ , red: O_2^+ , magenta: O^+ , and blue: CO_2^+), and panel (f) shows the density ratio of heavy ions (O^+ , O_2^+ , and CO_2^+) to H^+ ions.

the spacecraft (about -5.4 to -1 V). We focused on the period when the cold dense heavy ions were observed (indicated by red bar at the bottom of Figure 3).

Figure 4 is the enlarged figure of the period indicated by the red bar in Figure 3. At about 15:11 UT, MAVEN crossed the current sheet from the south dusk to north dawn lobes as shown in Figure 4a. Note that a flux rope was observed in the current sheet at this time (Hara et al., 2017). Number densities of heavy ions decreased significantly at the current sheet crossing around 15:11 UT. On the other hand, the H^+ number density is increased or almost constant at the crossing. Time variations of heavy ions were similar to each other, while H^+ variation was different, suggesting that H^+ ions have a different source or transport process. Therefore, there was a clear asymmetry between south dusk downward E and north dawn upward E hemispheres. The former was heavy ion dominant, and the latter was H^+ dominant.

In the period of cold dense (134 cm^{-3} on average) heavy ion outflow event (from 14:57 to 15:10), density ratio of heavy ions $O_2^+ : O^+ : CO_2^+$ is about 1:0.38:0.04. In other words, contribution of O_2^+ , O^+ , and CO_2^+ to total heavy ions (the sum of these three ion species) is about 71%, 26%, and 3%, respectively.

4. Discussion

Figure 5 illustrated outline of the cold dense heavy ion outflow event reported in this study. During the event, the strong crustal magnetic fields were located on the dayside, and cold dense heavy ions were observed only in south dusk downward E lobe. Mitchell et al. (2001) showed that the interaction between the solar

3. Results

The cold dense ion outflow with the peak O_2^+ density of $> 100 \text{ cm}^{-3}$ is observed in the Martian-induced magnetotail at the altitude of about 2,000 km around 15 UT on 4 December 2014 (orbit #354). Note that because of the limited field of view of the STATIC instrument, observed densities may be underestimates. However, derived total ion density agrees with electron density obtained by Langmuir Probe and Waves (Andersson et al., 2015) within 10% difference. As shown in Figure 2, MAVEN traverses the wake region from south dusk to north dawn quadrants. During the event, the strong crustal magnetic fields were located on the dayside of Mars.

In the same orbit, MAVEN also observed the solar wind region, and the interplanetary magnetic field was directed to approximately $+Y$ direction in Mars-Sun-Orbital (MSO) coordinate (X : Sun direction, Y : dusk direction, and Z : $X \times Y$ direction; ($B_x = -0.9$, $B_y = 2.9$, and $B_z = 1.3$ [nT], respectively). Therefore, based on a simple assumption that the current sheet direction is perpendicular to the projected interplanetary magnetic field on the Y - Z plane, the angle between the current sheet and X - Z plane in the MSO coordinates was about 24° . In other words, the solar wind electric field was tilted at 24° from Z axis in the MSO coordinates (as shown in Figure 2b).

In this period, MAVEN first observed the sheath region and then penetrated into the induced magnetotail. In the magnetotail optical wake region from 14:57 to 15:17 UT, cold dense heavy ions were observed even at high altitudes as shown in Figures 3b and 3c. Dense ionospheric ions were observed near the periapsis. After the periapsis, MAVEN passed by the sheath and solar wind regions. The sign of $X_{M_{SO}}$ component of magnetic field changed dramatically at about 15:11 UT, indicating that MAVEN passed by a current sheet. In the sheath and solar wind regions, H^+ and He^{++} ions were dominant populations with energies about 1 keV. In the induced magnetotail observed from 14:57 to 15:17 UT, heavy ions were observed. We could observe cold heavy ions in the wake region because of negative charging of

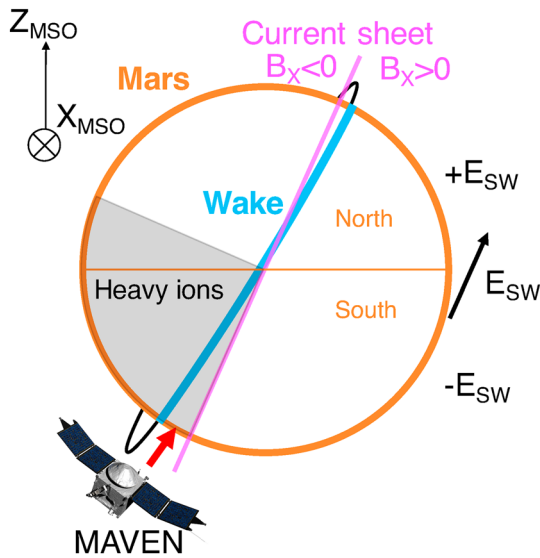


Figure 5. Schematic summary of cold dense ion outflow event on 4 December 2014, viewed from the tail region. Black line is a trajectory of the spacecraft, and in the period of light blue line, the spacecraft was in the wake region. Magenta line shows current sheet. Because of IMF condition, direction of E_{SW} is determined as the black arrow displayed in the figure. Black shaded region represents south dusk downward E lobe where cold dense heavy ions were observed. IMF = interplanetary magnetic field.

wind and the strong crustal magnetic fields forms the minimagnetosphere. Some of the crustal magnetic fields are “open” fields, one end connects to Mars, and the other end connects to tailward (Luhmann et al., 2015). A possible scenario of the ion outflow formation is that ionospheric heavy ions in this minimagnetosphere are gradually transported upward along the magnetic field lines in the cusp-like regions and flow out to the magnetotail.

In upward E hemisphere, heavy ions can be accelerated by the upward electric field induced by the solar wind and strong plumes can occur (Dong et al., 2015). Due to the flux conservation at high altitude, the strong acceleration results in lower density and higher velocity in the upward E hemisphere. Moreover, the efficient acceleration of plume ions in the upward E hemisphere makes their escape path more poleward and makes it difficult for them to reach such a near-Mars magnetotail region. Therefore, the observed decrease in the cold heavy ion densities from south downward E to north upward E hemisphere might be explicable with less acceleration in the downward E hemisphere.

The obtained number density ratios between heavy ion species provide us a clue to infer the source altitude of the cold dense ion outflow (e.g., Lundin et al., 2009). Roughly speaking, CO_2^+ originates from low altitudes. The ions obtained in the tail region can include light ion species coming from high altitudes, which suggests that the ratio of CO_2^+ decreases. Thus, the source altitude of ion outflow is expected to be lower than the altitude indicated by the ratio obtained

in the tail region. Withers et al. (2015) showed the ion density profiles observed by Neutral Gas and Ion Mass Spectrometer (Mahaffy et al., 2015) onboard MAVEN. Their results indicated that above 300 km, densities of O^+ ions and O_2^+ ions are comparable, and contribution of CO_2^+ to total heavy ions is smaller than 3%. Comparison with their results also indicates that the density ratio of heavy ions in the cold ion outflow, $O_2^+ : O^+ : CO_2^+$ (1:0.38:0.04), is almost the same as the density ratio at around 260-km altitude in the Martian ionosphere. Thus, it is suggested that the source altitude of heavy ions is around 260 km or below, considering possible addition of the lighter ions at altitudes higher than the source. If the minimagnetosphere was formed due to the existence of strong crustal magnetic fields, heavy ions at the low altitude could flow out more easily along the magnetic field lines. Formation of minimagnetosphere with cusps as well as less acceleration in downward E hemisphere might cause the cold dense ion outflow from the low-altitude ionosphere.

In this cold dense heavy ion outflow event, average flux of heavy ions was about $5.4 \times 10^7 \text{ cm}^{-2} \text{ s}^{-1}$. Note that it is challenging to derive the precise velocity due to the negative charging of spacecraft. Therefore we assume that all ions have the same velocity, that is, the escape velocity at altitude of 2,000 km from Mars. Considering that we observed the same outflow from the south dusk downward E quadrant (shaded area in Figure 5), we can obtain the total ion escape rate to be about $5 \times 10^{24} \text{ s}^{-1}$. This escape rate is not small compared to the previous statistical observations (e.g., $3.9 \times 10^{23} \text{ s}^{-1}$ in Barabash et al., 2007, $2.0 \times 10^{24} \text{ s}^{-1}$ in Nilsson et al., 2011, and $3 \times 10^{24} \text{ s}^{-1}$ in Brain et al., 2015), and contribution of this kind of cold ion outflows through the magnetotail is not negligible when one considers the total atmospheric escape from Mars. It should be noted that low-energy component normally dominates at the distances where the cold ion outflows were observed (Nilsson et al., 2012), and we could observe cold ions due to the negative charging of spacecraft.

5. Conclusion

In this paper, we report on the cold dense heavy ion outflow event observed by MAVEN on 4 December 2014 in the induced magnetotail wake region. In this event, cold dense ion outflow was observed only in south dusk downward E lobe. Strong local crustal magnetic field was located on the dayside in the period of this event. It might indicate that the cusp outflow from the minimagnetosphere formed by the interaction between the solar wind and the strong crustal magnetic fields facilitates the cold dense heavy ion outflow.

In other words, the spacecraft might be on open crustal field lines that have access to the low-altitude ionosphere when the spacecraft was in the southern hemisphere, and the escape in analogy with terrestrial case can occur by the mechanism such as ambipolar electric fields in cusp regions (André & Yau, 1997). The asymmetry of heavy ion density between the downward and upward E lobes in the Mars-Sun-Electric field coordinates is most likely to be caused by the solar wind electric field.

To obtain the number density of CO_2^+ ions, contamination from O_2^+ ions is eliminated by using a fitting method. The result shows that the relative contributions of O_2^+ , O^+ , and CO_2^+ to the heavy ion outflow are $\sim 71\%$, 26% , and 3% , respectively. Comparison with the density altitude profile in the Martian ionosphere suggests that the source altitude of the cold dense ion outflow is around 260 km or below. The estimated escape rate of heavy ions including CO_2^+ due to the cold ion outflow is about $5 \times 10^{24} \text{ s}^{-1}$. This value is not so small compared to previously reported other escape processes. The derivation method of CO_2^+ density developed in this study will be also applicable for the long-term MAVEN data to better understand statistical properties of various ion outflows for individual species from Mars.

Acknowledgments

This work was supported by Grant-in-Aid for Scientific Research (a) 16H02229 and (b) 15H03731 by Japan Society for the Promotion of Science (JSPS). The MAVEN project is supported by NASA Mars Exploration Program. The MAVEN data are available in NASA Planetary Data System. We are grateful to all MAVEN mission team members.

References

- Acuña, M. H., Connerney, J. E. P., Ness, N. F., Lin, R. P., Mitchell, D., Carlson, C. W., et al. (1999). Global distribution of crustal magnetization discovered by the Mars Global Surveyor MAG/ER experiment. *Science*, *284*(5415), 790–793. <https://doi.org/10.1126/science.284.5415.790>
- Andersson, L., Ergun, R. E., Delory, G. T., Eriksson, A., Westfall, J., Reed, H., et al. (2015). The Langmuir Probe and Waves (LPW) instrument for MAVEN. *Space Science Reviews*, *195*(1–4), 173–198. <https://doi.org/10.1007/s11214-015-0194-3>
- André, M., & Yau, A. (1997). Theories and observations of ion energization and outflow in the high latitude magnetosphere. *Space Science Reviews*, *80*(1/2), 27–48. <https://doi.org/10.1023/A:1004921619885>
- Barabash, S., Fedorov, A., Lundin, R., & Sauvaud, J.-A. (2007). Martian atmospheric erosion rates. *Science*, *315*(5811), 501–503. <https://doi.org/10.1126/science.1134358>
- Bibring, J.-P., Langevin, Y., Mustard, J. F., Poulet, F., Arvidson, R., Gendrin, A., et al. (2006). Global mineralogical and aqueous Mars history derived from OMEGA/Mars express data. *Science*, *312*(5772), 400–404. <https://doi.org/10.1126/science.1122659>
- Brain, D. A., Baker, A. H., Briggs, J., Eastwood, J. P., Halekas, J. S., & Phan, T.-D. (2010). Episodic detachment of Martian crustal magnetic fields leading to bulk atmospheric plasma escape. *Geophysical Research Letters*, *37*, L14108. <https://doi.org/10.1029/2010GL043916>
- Brain, D. A., McFadden, J. P., Halekas, J. S., Connerney, J. E. P., Bougher, S. W., Curry, S., et al. (2015). The spatial distribution of planetary ion fluxes near Mars observed by MAVEN. *Geophysical Research Letters*, *42*, 9142–9148. <https://doi.org/10.1002/2015GL065293>
- Carlsson, E., Fedorov, A., Barabash, S., Budnik, E., Grigoriev, A., Gunell, H., et al. (2006). Mass composition of the escaping plasma at Mars. *Icarus*, *182*(2), 320–328. <https://doi.org/10.1016/j.icarus.2005.09.020>
- Chassefière, E., & Leblanc, F. (2004). Mars atmospheric escape and evolution: Interaction with the solar wind. *Planetary and Space Science*, *52*(11), 1039–1058. <https://doi.org/10.1016/j.pss.2004.07.002>
- Connerney, J. E. P., Acuña, M. H., Ness, N. F., Kletetschka, G., Mitchell, D. L., Lin, R. P., & Rème, H. (2005). Tectonic implications of Mars crustal magnetism. *Proceedings of the National Academy of Sciences of the United States of America*, *102*(42), 14,970–14,975. <https://doi.org/10.1073/pnas.0507469102>
- Connerney, J. E. P., Espley, J., Lawton, P., Murphy, S., Odom, J., Oliverson, R., & Sheppard, D. (2015). The MAVEN magnetic field investigation. *Space Science Reviews*, *195*(1–4), 257–291. <https://doi.org/10.1007/s11214-015-0169-4>
- Dong, Y., Fang, X., Brain, D. A., McFadden, J. P., Halekas, J. S., Connerney, J. E., et al. (2015). Strong plume fluxes at Mars observed by MAVEN: An important planetary ion escape channel. *Geophysical Research Letters*, *42*, 8942–8950. <https://doi.org/10.1002/2015GL065346>
- Fang, X., Ma, Y., Brain, D., Dong, Y., & Lillis, R. (2015). Control of Mars global atmospheric loss by the continuous rotation of the crustal magnetic field: A time-dependent MHD study. *Journal of Geophysical Research: Space Physics*, *120*, 10,926–10,944. <https://doi.org/10.1002/2015JA021605>
- Halekas, J. S., Ruhunusiri, S., Harada, Y., Collinson, G., Mitchell, D. L., Mazelle, C., et al. (2017). Structure, dynamics, and seasonal variability of the Mars-solar wind interaction: MAVEN solar wind ion analyzer in-flight performance and science results. *Journal of Geophysical Research: Space Physics*, *122*, 547–578. <https://doi.org/10.1002/2016JA023167>
- Halekas, J. S., Taylor, E. R., Dalton, G., Johnson, G., Curtis, D. W., McFadden, J. P., et al. (2015). The solar wind ion analyzer for MAVEN. *Space Science Reviews*, *195*(1–4), 125–151. <https://doi.org/10.1007/s11214-013-0029-z>
- Hara, T., Harada, Y., Mitchell, D. L., DiBraccio, G. A., Espley, J. R., Brain, D. A., et al. (2017). On the origins of magnetic flux ropes in near-Mars magnetotail current sheets. *Geophysical Research Letters*, *44*, 7653–7662. <https://doi.org/10.1002/2017GL073754>
- Jakosky, B. M., Lin, R. P., Grebowsky, J. M., Luhmann, J. G., Mitchell, D. F., Beutelschies, G., et al. (2015). The Mars Atmosphere and Volatile Evolution (MAVEN) mission. *Space Science Reviews*, *195*(1–4), 3–48. <https://doi.org/10.1007/s11214-015-0139-x>
- Jakosky, B. M., & Phillips, R. J. (2001). Mars' volatile and climate history. *Nature*, *412*(6843), 237–244. <https://doi.org/10.1038/35084184>
- Lillis, R. J., Brain, D. A., Bougher, S. W., Leblanc, F., Luhmann, J. G., Jakosky, B. M., et al. (2015). Characterizing atmospheric escape from Mars today and through time, with MAVEN. *Space Science Reviews*, *195*(1–4), 357–422. <https://doi.org/10.1007/s11214-015-0165-8>
- Luhmann, J. G., Dong, C., Ma, Y., Curry, S. M., Mitchell, D., Espley, J., et al. (2015). Implications of MAVEN Mars near-wake measurements and models. *Geophysical Research Letters*, *42*, 9087–9094. <https://doi.org/10.1002/2015GL066122>
- Lundin, R., Barabash, S., Fedorov, A., Holmström, M., Nilsson, H., Sauvaud, J.-A., & Yamauchi, M. (2008). Solar forcing and planetary ion escape from Mars. *Geophysical Research Letters*, *35*, L09203. <https://doi.org/10.1029/2007GL032884>
- Lundin, R., Barabash, S., Holmström, M., Nilsson, H., Yamauchi, M., Dubinin, E. M., & Fraenz, M. (2009). Atmospheric origin of cold ion escape from Mars. *Geophysical Research Letters*, *36*, L17202. <https://doi.org/10.1029/2009GL039341>
- Lundin, R., Barabash, S., Yamauchi, M., Nilsson, H., & Brain, D. (2011). On the relation between plasma escape and the Martian crustal magnetic field. *Geophysical Research Letters*, *38*, L02102. <https://doi.org/10.1029/2010GL046019>
- Mahaffy, P. R., Benna, M., Elrod, M., Yelle, R. V., Bougher, S. W., Stone, S. W., & Jakosky, B. M. (2015). Structure and composition of the neutral upper atmosphere of Mars from the MAVEN NGIMS investigation. *Geophysical Research Letters*, *42*, 8951–8957. <https://doi.org/10.1002/2015GL065329>

- McFadden, J. P., Kortmann, O., Curtis, D., Dalton, G., Johnson, G., Abiad, R., et al. (2015). MAVEN SupraThermal and Thermal Ion Composition (STATIC) instrument. *Space Science Reviews*, 195(1-4), 199–256. <https://doi.org/10.1007/s11214-015-0175-6>
- Mitchell, D. L., Lin, R. P., Mazelle, C., Rème, H., Cloutier, P. A., Connerney, J. E. P., et al. (2001). Probing Mars' crustal magnetic field and ionosphere with the MGS Electron Reflectometer. *Journal of Geophysical Research*, 106, 23,419–23,427. <https://doi.org/10.1029/2000JE001435>
- Morschhauser, A., Lesur, V., & Grott, M. (2014). A spherical harmonic model of the lithospheric magnetic field of Mars. *Journal of Geophysical Research: Planets*, 119, 1162–1188. <https://doi.org/10.1002/2013JE004555>
- Nilsson, H., Carlsson, E., Brain, D. A., Yamauchi, M., Holmström, M., Barabash, S., et al. (2010). Ion escape from Mars as a function of solar wind conditions: A statistical study. *Icarus*, 206(1), 40–49. <https://doi.org/10.1016/j.icarus.2009.03.006>
- Nilsson, H., Edberg, N. J. T., Stenberg, G., Barabash, S., Holmström, M., Futaana, Y., et al. (2011). Heavy ion escape from Mars, influence from solar wind conditions and crustal magnetic fields. *Icarus*, 215(2), 475–484. <https://doi.org/10.1016/j.icarus.2011.08.003>
- Nilsson, H., Stenberg, G., Futaana, Y., Holmström, M., Barabash, S., Lundin, R., et al. (2012). Ion distributions in the vicinity of Mars: Signatures of heating and acceleration processes. *Earth, Planets and Space*, 64(2), 135–148. <https://doi.org/10.5047/eps.2011.04.011>
- Ramirez, R. M., Koppapu, R., Zuger, M. E., Robinson, T. D., Freedman, R., & Kasting, J. F. (2014). Warming early Mars with CO₂ and H₂. *Nature Geoscience*, 7(1), 59–63. <https://doi.org/10.1038/ngeo2000>
- Ramstad, R., Barabash, S., Futaana, Y., Nilsson, H., & Holmström, M. (2016). Effects of the crustal magnetic fields on the Martian atmospheric ion escape rate. *Geophysical Research Letters*, 43, 10,574–10,579. <https://doi.org/10.1002/2016GL070135>
- Soobiah, Y., Coates, A. J., Linder, D. R., Kataria, D. O., Winningham, J. D., Frahm, R. A., et al. (2006). Observations of magnetic anomaly signatures in Mars Express ASPERA-3 ELS data. *Icarus*, 182(2), 396–405. <https://doi.org/10.1016/j.icarus.2005.10.034>
- Trotignon, J. G., Mazelle, C., Bertucci, C., & Acuña, M. H. (2006). Martian shock and magnetic pile-up boundary positions and shapes determined from the Phobos 2 and Mars Global Surveyor data sets. *Planetary and Space Science*, 54, 357–369. <https://doi.org/10.1016/j.pss.2006.01.003>
- Withers, P., Vogt, M., Mayyasi, M., Mahaffy, P., Benna, M., Elrod, M., et al. (2015). Comparison of model predictions for the composition of the ionosphere of Mars to MAVEN NGIMS data. *Geophysical Research Letters*, 42, 8966–8976. <https://doi.org/10.1002/2015GL065205>